Experimental Cell Research 361 (2017) 9–18

Contents lists available at ScienceDirect

Experimental Cell Research

journal homepage: www.elsevier.com/locate/yexcr

IGF-I regulates HT1080 fibrosarcoma cell migration through a syndecan-2/Erk/ezrin signaling axis

Maria Mytilinaiou[a], Dragana Nikitovic[a], Aikaterini Berdiaki[a], Antonis Papoutsidakis[a], Dionysios J. Papachristou[b], Aristidis Tsatsakis[c], George N. Tzanakakis[a,*]

[a] Laboratory of Anatomy-Histology-Embryology, School of Medicine, University of Crete, 71003 Heraklion, Greece
[b] Laboratory of Toxicology, School of Medicine, University of Crete, 71003 Heraklion, Greece
[c] Laboratory of Anatomy-Histology-Embryology, Unit of Bone and Soft Tissue Studies, School of Medicine, University of Patras, Patras, Greece

ARTICLE INFO

Keywords:
Fibrosarcoma
Syndecan 2
Insulin-like growth factor receptor
Ezrin
Cell migration

ABSTRACT

Fibrosarcoma is a tumor of mesenchymal origin, originating from fibroblasts. IGF-I is an anabolic growth factor which exhibits significant involvement in cancer progression. In this study, we investigated the possible participation of syndecan-2 (SDC-2), a cell membrane heparan sulfate (HS) proteoglycan on IGF-I dependent fibrosarcoma cell motility. Our results demonstrate that SDC-2-deficient HT1080 cells exhibit attenuated IGF-I-dependent chemotactic migration ($p < 0.001$). SDC-2 was found to co-localize to IGF-I receptor (IGF-IR) in a manner dependent on IGF-I activity ($P \leq 0.01$). In parallel, the downregulation of SDC-2 significantly inhibited both basal and due to IGF-I action ERK1/2 activation, ($p < 0.001$). The phosphorylation levels of ezrin (Thr567), which is suggested to act as a signaling bridge between the cellular membrane receptors and actin cytoskeleton, were strongly enhanced by IGF-I at both 1 h and 24 h ($p < 0.05$; $p < 0.01$). The formation of an immunoprecipitative complex revealed an association between SDC2 and ezrin which was enhanced through IGF-I action ($p < 0.05$). Immunoflourescence demonstrated a co-localization of IGF-IR, SDC2 and ezrin upregulated by IGF-I action. **IGF-I enhanced actin polymerization and ezrin/actin specific localization to cell membranes.** Finally, treatment with IGF-I strongly increased SDC2 expression at both the mRNA and protein level ($p < 0.001$). Therefore, we propose a novel SDC2-dependent mechanism, where SDC2 is co-localized with IGF-IR and enhances its' IGFI-dependent downstream signaling. SDC2 mediates directly IGFI-induced ERK1/2 activation, it recruits ezrin, *contributes to actin polymerization and ezrin/actin specific localization to cell membranes,* ultimately facilitating the progression of IGFI-dependent fibrosarcoma cell migration.

1. Introduction

Fibrosarcoma is a tumor of mesenchymal origin, predominantly derived from malignant spindle fibroblasts. Recent epidemiologic data ranks fibrosarcoma as with lowest incidence in the soft tissue tumor list. The reason for this development in fibrosarcoma identification is the increased sensitivity of the histopathology-based classification system, leading to more accurate diagnosis [1,2]. The relatively low frequency of fibrosarcoma has resulted in a limited number of research reports, aimed at the identification of specific therapeutic targets for this disease. However, despite its low incidence, adult fibrosarcoma is reported to have a very poor prognosis [3,4] which highlights the necessity for the development of new therapies. Growth factors (GFs) have been indicated in fibrosarcoma progression [5–9]. However, only a few of the complex cellular networks, through which GFs affect fibrosarcoma progression, have been clarified so far. The purpose of this study therefore was the detection of target signaling mediators, which regulate cell migration, crucial to high fibrosarcoma metastatic ability.

IGF-I is an anabolic growth factor that has been extensively studied [10]. Recent reports have shown that apart from its well-known growth hormone (GH)-dependent roles, either through hepatic or other target tissue production, IGF-I is also demonstrated to have GH-independent properties on specific target sites [11]. Importantly, IGF-I not only has major physiological effects on growth, but it exhibits a significant involvement in cancer progression [12]. Indeed, individuals with high levels of IGF-I, either acromegalic, obese or type 2 diabetic patients have increased risk of developing certain types of cancer. On the contrary, patients who have IGF-I deficiency, such as patients with Laron syndrome (congenital IGF-I deficiency and GH insensitivity) and patients with congenital isolated GH deficiency are protected from developing cancer, as compared to their healthy relatives [13]. Many illuminating studies assessing the carcinogenic effects of IGF-I have been performed [13,14].

* Correspondence to: Faculty of Medicine, University of Crete, 71003 Voutes, Heraklion, Greece.
E-mail address: tzanakak@uoc.gr (G.N. Tzanakakis).

http://dx.doi.org/10.1016/j.yexcr.2017.09.035
Received 22 May 2017; Received in revised form 15 September 2017; Accepted 25 September 2017
Available online 28 September 2017
0014-4827/

Indeed, at the cell level, it has been shown that IGF-I promotes tumorigenesis by inhibiting apoptosis and promoting cell cycle progression as well as angiogenesis [15–18]. Numerous studies, have established the role of IGF-I in cancer metastasis [19–22]. The effects of IGF-I are mainly mediated through its receptor IGF-IR and its bioavailability is controlled by the respective binding proteins (IGFBPs). Up to date 6 IGFBPs have been identified, with IGFBP-3 being the most abundant in the blood [12,17,23]. Upon IGF-IR activation key intracellular signaling pathways, including the MAP and PI3 kinase pathways, are initialized [16,18,24]. These signaling pathways have been demonstrated to play an important role in cancer progression as shown in the case of ERK1/2 [25–27]. Indeed, IGF-IR silencing suppresses epithelial-mesenchymal transition (EMT), a process which is crucial for the invasive properties of the tumor, through inhibition of PI3K/AKT, MEK/ERK and JAK/STAT signaling [28]. Furthermore, interactions with endothelial growth factor receptor (EGFR) and estrogen receptors (ERs) have been attributed to IGF-IR during tumorigenesis [29,30].

Research efforts have shown that IGF-I has a significant effect on both epithelial and mesenchymal derived tumors [14,15,18,31]. The effect of IGF-I on tumors of mesenchymal origin was highlighted in an early animal study, when growth hormone (GH)- IGF-I axis was shown to drive the formation of fibrosarcoma metastases in rats [19]. These studies raised the hypothesis that IGF/IGF-IR antagonists could be potential therapeutic agents. Indeed, the use of monoclonal antibodies against IGF-IR in the case of osteosarcoma, rhabdomyosarcoma and especially on Ewing sarcoma has shown satisfactory results [32,33].

Syndecans (SDCs) are a family of four cell surface heparan sulfate proteoglycans exhibiting a plethora of roles with regards to the regulation of “in-out” and “out-in” signaling. SDC-dependent signaling affects crucial cell functions including cell-matrix adhesion and motility [34–37]. Importantly, the SDC2 member is highly expressed in mesenchymal cells where it regulates these cells’ motility [38–40]. Overexpression of SDC2 in HT1080 fibrosarcoma cells was demonstrated to facilitate these cells' migration through a FAK/PI3K/rac signaling pathway [38]. Intriguingly, syndecan 1 (SDC1) was found to induce IGF-IR activation in a SDC2-dependent manner in fibrosarcoma cells [41]. The present study thus, hypothesized the putative association of SDC2 and IGF-1-signaling in the regulation of HT1080 cell motility. Our novel results demonstrate that IGF-1/IGF-IR through a SDC2/ezrin/Erk mechanism upregulate actin cytoskeleton organization to facilitate HT1080 cell migration.

2. Materials and methods

2.1. Cell culture

For the purposes of this study, the human fibrosarcoma HT1080 and B6FS cell human fibrosarcoma cell lines were used used [42,43]. HT1080 cells were incubated at 37 °C and 5% v/v CO_2, in culture flasks, or plates with the relevant substrate. They were grown in Dulbecco's Modified Eagle Medium (DMEM) (Biochrom, KG, Germany) supplemented with fetal bovine serum (FBS) 10% (v/v) (Gibco, CA), glutamine (4 mM), penicillin (100units/ml) and streptomycin (100 μg/ml). Prior to treatment with IGFI (5 ng/ml) for a 24 h period, cells were cultured in serum-free DMEM for 24 h. *B6FS human fibrosarcoma cell line [43] was obtained from the Cell Bank of the Karolinska Institute, Stockholm, Sweden and was a kind gift from Dr. Anders Hjerpe (Karolinska Institute). B6FS cells were cultured at* 37 °C *and humidity* 5% CO_2 *in RPMI supplemented with* 10% *FBS and antimicrobial agents* (100 IU/ml *penicillin,* 100 μg/ml *streptomycin and* 0.5% *gentamycin). Prior to treatment with IGFI* (5 ng/ml) *the cells were cultured under serum-free conditions during* 24 h.

2.2. RNA Isolation and real-time PCR

The TRIzol method (Gibco) and the DyNAmo cDNA synthesis kit (Finnzymes, Vantaa, Finland) were used for mRNA extraction and cDNA synthesis, respectively. Five micrograms of total RNA were used for cDNA synthesis according to the manufacturer's instructions. Primers were mRNA specific in order to avoid results from DNA contamination traces (SDC-2: F-5′-GGGAGCTGATGAGGATGTAG-3′, R-5′-CACTGGATGGTTTGCGTTCT-3′; GAPDH: F-5′ GGAAGGTGAAGGTCG GAGTCA-3′, R-5′- GTCATTGATGGCAACAATATCCACT-3′; EZRIN: F-5′-GTTTTCCCCAGTTGTAATAGT GCC-3′ R-5′-TCCGTAATTCAATCAGT CCTGC-3′; IGF-IR: F-5′-TCTCTTCTACCTGGCGCTGT-3′, R-5′-AAGCA GCAGTCATCCACGAT-3′). For the real-time polymerase chain reaction (PCR) reaction QuantiTech SYBR Green master mix (Qiagen, CA) was used (total 20 μl reaction volume) and performed by an M3300P cycler. Standard curves were run in each optimized assay which produced a linear plot of threshold cycle (Ct) against log (dilution). The quantity of each target was normalized against the quantity of glyceraldehyde-3-phosphate dehydrogenase (GAPDH) and was presented as arbitrary units as previously described [5].

2.3. Western blotting

Cells were harvested after specific treatments, using Radio Immunoprecipitation Assay Buffer (RIPA) solution. The samples were electrophoresed on 8% polyacrylamide Tris/Glycine gels and transferred to nitrocellulose membranes (10 mM (3-(cyclohexylamino) − 1-propanesulfonic acid [CAPS] by Sigma, St. Louis, MO), pH 11, containing 10% methanol). Membranes were blocked overnight at 4 °C with PBS containing 0.1%Tween-20 (PBS-T) and 5% (w/v) low-fat milk powder. Next day, membranes were incubated for 1 h at room temperature (RT) with primary antibodies (SantaCruz, CA), anti-P-ERK, (1:100), anti-ERK (1:200), anti-actin (1:200), anti-SDC-2 (1:200), anti-ezrin (1:500) and anti-p-ezrin (1:200). The immune complexes were detected after incubation with the appropriate peroxidase-conjugated secondary antibody (1:3000) with the SuperSignalWest Pico Chemiluminescent substrate (Pierce, IL), according to the manufacturer's instructions.

2.4. Transfection with siRNA

Short interfering RNA (siRNA) specific for SDC-2 and a scrambled siRNA as a negative control were purchased from Invitrogen, USA. Transfection was performed as previously described [5]. Briefly, HT1080 **and B6FS** cells (6×10^4/well) were placed on a 24-well plate for 24 h. To provide for optimal transfection, siRNA (100 nM; Invitrogen) and Lipofectamine 2000 (1 μl; Invitrogen) were first diluted separately in 50 μlOpti-MEM I Reduced Serum Medium (Invitrogen). After a 5-min incubation period, 50 μl diluted Lipofectamine 2000 was mixed with 50 μl diluted siRNA per well on 24-well plates and were left for 20 min at room temperature to allow siRNA–liposome complexes to form. Cells were detached using trypsin-EDTA which was deactivated with 10% serum medium. The cells were then washed with serum and antibiotics-free medium, counted and added on top of the lipofectamine and siRNA mix and shaken gently. Transfection was allowed to take place during a 6 h period when the medium was replaced with fresh serum-free medium containing antibiotics and treatments were performed for further 48 h. At this time point, the cells were harvested and RNA was extracted. All transfection experiments were repeated at least three times and performed in triplicates.

2.5. Immunofluorescence

HT1080 cells were seeded on round coverslips placed in 24-well plates in 10% serum DMEM followed by a 24 h period of serum starvation. At this point, treatments were added, and the cells were incubated for another 24 h period. Afterwards, the cells were fixed and permeabilized before the addition of primary anti-SDC2 antibody (1:50), primary anti-ezrin antibody (1:50), primary anti-p-ezrin antibody and primary anti-IGFI-R antibody for 1 h at RT. The coverslips

were incubated for 1 h, in the dark at RT, with anti-goat Alexa Fluor 488 (Invitrogen). TO-PRO-3 diluted 1:1000 in deionized H_2O was applied for 10 min to stain nuclei as previously reported [30,44]. Actin filaments were detected using fluorescent phalloidin (Molecular Probes) diluted 1:100 in PBS for 40 min as previously reported [30,45]. The coverslips were then placed onto slides using glycerol as a mount solution and visualized using confocal microscopy.

2.6. Cell migration assay

The ability of the cells to migrate was analyzed using a cell chemotaxis assay [46,47]. The cells were grown as described above. After treatment and harvesting with PBS/EDTA, 5×10^4 cells were diluted into a volume of 300 μl DMEM 0% and finally placed on the upper chamber of Trans-well inserts (8 μm polycarbonate membrane; 6.5 mm insert), in a 24 well (Costar), while in the lower chamber, fibronectin was used (10 μg/ml) as chemoattractant in 500 μl DMEM 0%. After 4 h, the cells that had penetrated the semi-permeable membrane were harvested with trypsin solution and quantified with CyQUANT cell proliferation AssayKit (MolecularProbes) using a fluorometer, according to the manufacturer's instructions. **Shortly, cell media was removed whereupon the cells were lysed by freezing and** the **DNA content measured through fluorescent dye binding. A standard curve was used to convert fluorescence units to cell numbers. All measurements were performed in triplicates.**

2.7. Immunoprecipitation

For immunoprecipitation with protein A/G and agarose, cells were diluted in 1 ml NP40, which contained protease inhibitors and phosphatases. 100 μl from this dilution were frozen in −80 °C. In the rest 900 μl of every protein sample, 30 μl of the primary antibody was added and was centrifuged gently overnight at 4 °C (3 μg of primary antibody for 1 mg of total protein). The next day, 30 μl of protein A/G with agaroze (SantaCruz) was added for 4 h at 4 °C. After centrifugation at 1000 rpm for 1 min (4 °C), the precipitate was diluted again with 1 ml NP40. This process was repeated twice more. Finally, the precipitate was diluted in 30 μl 2x dye and the samples were utilized for Western blot analysis as previously reported [44].

2.8. Statistical analysis

The statistical tests used for data analysis were: ANOVA, Chi-square και Student's T. Statistical significance was considered as $p < 0.05$.

3. Results

3.1. IGFI regulates HT1080 cell migration in a SDC2-dependent manner

In the present study, the chemotactic migration of HT1080, poorly differentiated and highly aggressive human fibrosarcoma cells [42], was initially examined against fibronectin (FN) and Fetal Bovine Serum (FBS) utilizing DMEM (0%) as control. HT1080 cell exhibited enhanced migration towards FN and FBS (Fig. 1A). Treating HT1080 cells with IGF-I (5 ng/ml) during 24 h strongly increased their chemotactic migration towards FN and FBS, ($p < 0.01$ and $p < 0.001$), as compared to the respective control (Fig. 1A). Due to high prevalence of FN in fibrosarcoma extracellular matrix we utilized FN as a chemotactic agent in all subsequent experiments. SDC2 is abundant in mesenchymal cells, and was earlier demonstrated to affect HT1080 cell migration [38] in collaboration with syndecan 1 (SDC1) [41]. In order to investigate the putative role of SDC2 in IGFI-mediated HT1080 cell migration, we silenced the SDC2 gene expression by utilizing siRNA transfection, obtaining satisfactory downregulation of SDC2, as previously described [5]. As presented in Fig. 1B, SDC2 is necessary for IGF-induced cell migration, as SDC2-deficient cells treated with IGF-I exhibited

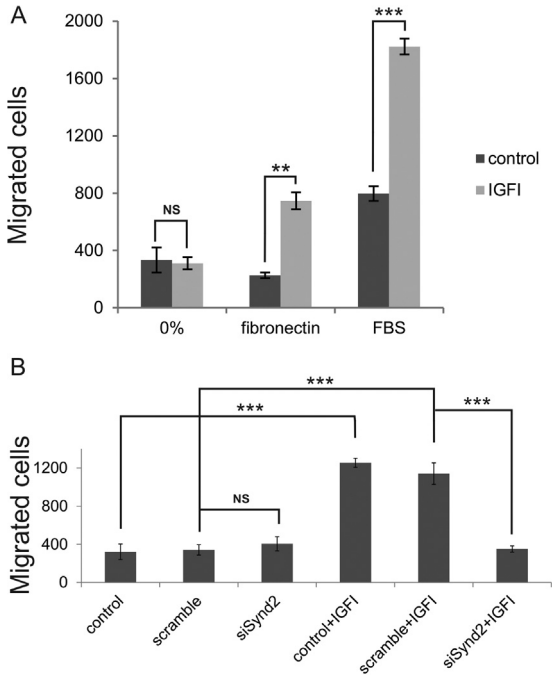

Fig. 1. IGFI regulates HT1080 cell migration in a SDC2-dependent manner. (A) HT1080 cells were treated with DMEM 0%, or IGFI (5 ng/ml) for 24 h before harvesting and re-seeding of 50×10^3 cells into 24-well plate inserts with 400 μl DMEM 0%. The lower chamber contained 500 μl DMEM 0%, 500 μl DMEM 0% plus 5 μl fibronectin, or 500 μl DMEM 0% plus FBS. Cells were then incubated at 37 °C for 4 h and left to migrate through the pores of the inserts, towards the chemoattractant. The migrating cells that passed into the lower chamber were harvested at this point utilizing 1 min treatment with 100 μl trypsin and kept in −70 °C for 24 h. The number of migrating cells was determined using fluorometric CyQUANT Assay Kit (Molecular Probes). The results represent the average of three separate experiments in triplicate. Means ± S.E.M. plotted; statistical significance: NS > 0.05, **p ≤ 0.01, ***p ≤ 0.001 treatment compared to control. (B) HT1080 cells were either transfected with siRNA specific for syndecan 2 (siSDC2), or control scramble RNA (siScr) and treated or not with IGFI (5 ng/ml) for 24 h before harvesting and re-seeding into the upper chambers of 24-well plate inserts. Cells were incubated for 4 h at 37 °C and left to migrate towards the fibronectin-coated lower chamber of the 24-well plate, via the pores of the inserts. The migrating cells that passed into the lower chamber were harvested at this point utilizing 1 min treatment with 100 μl trypsin and kept in −70 °C for 24 h. Fluorometric CyQUANT Assay Kit (Molecular Probes) was used as a method to assess the number of the migrating cells. The results represent the average of three separate experiments in triplicate. Means ± S.E.M. plotted; statistical significance: NS > 0.05, ***p ≤ 0.001 among samples.

significantly decreased ability to migrate as compared to the siScramble (siSCR) control ($p < 0.001$). *In parallel, the effects of IGF-I/SDC2 signaling were examined in B6FS cells. SDC2 does not affect these cells' motility as the downregulation of SDC2 expression* ($p < 0.001$), *did not affect the ability of SDC2-deficient, siSDC2, cells to migrate as compared to the siScr control* (p = NS) (Supplemental Figure 1A, B and C). *Treatment with IGF-I* (5 ng/ml) *during* 24 h *did not affect B6FS cells' chemotactic migration towards FN* (p = NS) *(Supplemental Figure 1C). According to these data, in continuation we focused on the mechanism of IGF-I/SDC2 action in HT1080 cells.*

In an attempt to map potential connections and pathways in IGFI-treated HT1080 cells and taking into account the postulated role of SDC2 in SDC1-dependent migration [41] we examined the possibility of SDC2 and IGF-IR co-localization in HT1080 cells. In this respect we utilized an antibody specific for IGF-IR for immunoprecipitation whereas we probed the complex with an anti-SDC2 Ig. As shown in Fig. 2A and B, SDC2 was found to be co-located to IGFI-R and this association was upregulated by IGF-I action ($p < 0.05$). Treatment with IGF-I decreased IGF-IR mRNA levels, did not affect IGF-IR expression at protein level, whereas an upregulation of IGF-IR phosphorylation was evident in IGF-I treated cells (Supplemental Figure 2A, B and C).

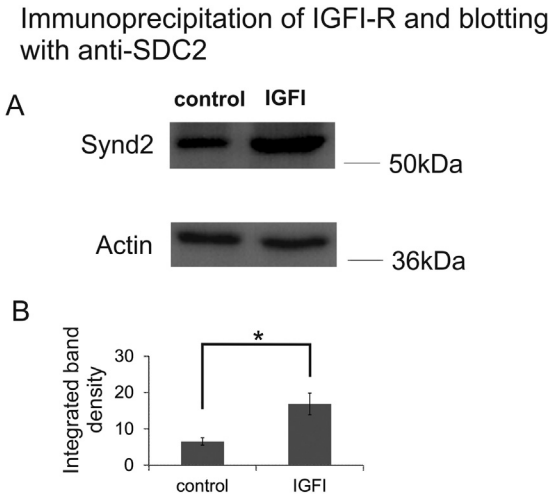

Fig. 2. SDC2 co-localizes with IGF-IR. HT1080 cells were treated with DMEM 0%, or with IGFI (5 ng/ml) for 24 h, whereupon they were harvested and cell extract proteins obtained. A. Western blot analysis was used for the visualization of SDC-2 protein expression in control cells treated with culture medium (control), samples treated with IGF-I and immunoprecipitated with anti-IGF-IR in the cell extracts stored from each sample (total protein) of the same experiment. B. Densitometric analysis of the bands was normalized against actin and plotted. The results represent the average of three separate experiments. Means ± S.E.M. plotted; statistical significance is as follows: *p ≤ 0.05 compared with the respective control samples.

3.2. SDC2 modulates IGFI-dependent ERK1/2 activation

Subsequently, we examined key IGF-I downstream mediators focusing on Extracellular signal Regulated Kinases1/2 (ERK1/2). Indeed, ERK1/2 is well established to be an IGF-I downstream conduit, not only in the regulation of protein expression, differentiation, EMT and cell proliferation, but also for tumor cell migration [48–52]. The utilization of a specific ERK1/2 inhibitor demonstrated a significant suppression of IGF-I-mediated migration ($p < 0.001$); whereas the basal migratory capacity of HT1080 cells was not affected (Fig. 3A). Thereupon, we examined whether there is a connection between SDC2 signaling and ERK1/2 activation. It has been shown previously that overexpression of SDC2 in HT1080 cells results in hyperphosphorylation of ERK1/2 [41]. To determine the effect of SDC2 on IGF-I-dependent ERK1/2 activation in HT1080 cells, we examined the ERK1/2 phosphorylation levels of both control and IGFI-treated SDC-2-deficient cells. As shown in Fig. 3B and C, SDC2 participation was found to be crucial for both the IGFI-induced and basal ERK1/2 phosphorylation as SDC2-deficient cells exhibited attenuated both basal and IGF-I –dependent ERK1/2 activation, ($p < 0.001$).

3.3. IGFI regulates ezrin activation

The next set of experiments aimed at determining the mechanisms through which IGF/SDC2 signaling affects HT1080 cell migration. We focused on ezrin, a molecule established to interact with SDC2 and induce changes to the cytoskeleton [53,54]. Ezrin is known to be partly activated through specific phosphorylation of Thr567, which induces conformational changes in the molecule and ultimately unmasks binding sites for F-actin, SDC2, as well as other binding partners [55,56]. Noteworthy, ezrin has been identified as a downstream modulator of IGF-IR signaling in colorectal cancer cells [57]. To explore the putative link between IGF-I signaling and ezrin activation we treated HT1080 cells with IGF-I and measured ezrin mRNA and protein expression as well as its phosphorylation levels (Thr567). As shown in Fig. 4A, IGF-I induced at the 24 h point a strong enhancement of ezrin mRNA ($p < 0.001$) which was not translated to increased protein expression (Fig. 4B). However, IGF-I strongly enhanced ezrin

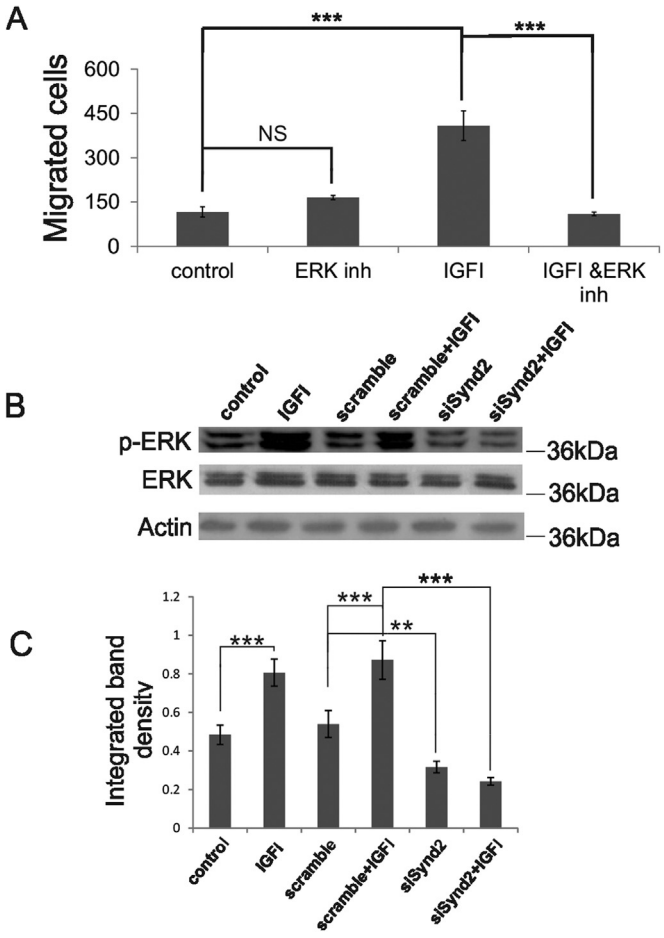

Fig. 3. SDC2 through IGFI-dependent ERK1/2 activation regulates cell migration. (A) HT1080 cells were treated with ERK inhibitor 1 h prior to the addition of IGFI. After 24 h, cells were harvested and reseeded into 24-well plate inserts, incubated for 4 h at 37 °C, and allowed to migrate to the fibronectin-containing lower chamber of the 24-well plate. The number of migrating cells was determined using fluorometric CyQUANT Assay Kit (Molecular Probes). The results represent the average of three separate experiments in triplicate. Means ± S.E.M. plotted; statistical significance: NS > 0.05, ***p ≤ 0.001 among samples. (B) HT1080 cells were either treated as control with DMEM 0% or with IGFI (5 ng/ml) for 24 h, harvested and equal amounts of cell extract protein were blotted against p-ERK1/2 specific antibody. Representative blots are presented. (C) Specific p-ERK1/2 protein bands were densitometrically analyzed and adjusted *against total ERK1/2 protein as well as actin.* The results represent the average of three separate experiments in triplicate. Means ± SEM plotted; Statistical significance *** p ≤0.001 among samples.

phosphorylation level (Thr567) at both 1 h and 24 h ($p < 0.05$; $p < 0.01$), respectively (Fig. 4B and C).

3.4. Formation of SDC2 / p-ezrin IP complex

It has been previously shown that SDC2 binds ezrin in fibroblast-like cells, facilitating these cells lamellipodia formation [53,54]. In order to investigate the putative interaction between SDC2 and ezrin in HT1080 cells we conducted an immunoprecipitation experiment (IP) on cells treated with IGF-I (5 ng/ml). The immunoprecipitation was performed with an antibody specific for p-ezrin and the complex was probed with an anti-SDC2 Ig. This approach resulted in the formation of an immunoprecipitative complex revealing an association between these two molecules which was enhanced through IGF-I action ($p < 0.05$) (Fig. 5A and B).

3.5. IGF-I facilitates SDC2/ezrin and SDC2/IGF-IR associations

To visualize SDC2/ezrin associations and to examine putative

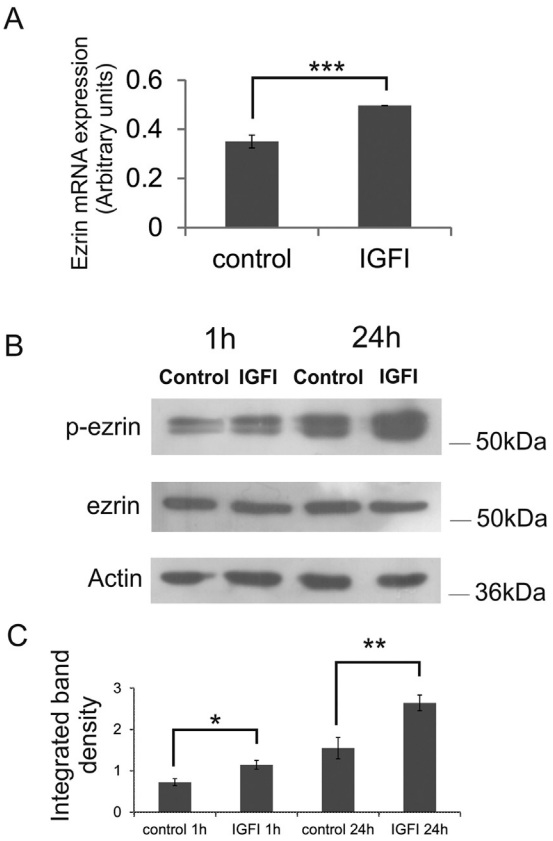

Fig. 4. IGFI regulates ezrin expression and activation. (A) Expression of ezrin was quantified by Real-time PCR, after treating HT1080 cells with DMEM 0%, or IGFI (5 ng/ml) for 24 h. The results represent the average of three separate experiments in triplicate. Means ± S.E.M plotted; Statistical significance ***p ≤ 0.001 among control and respective treatments. (B) HT1080 cells, either as control with DMEM 0%, or treated with IGFI (5 ng/ml) for 1 h and 24 h, were harvested and equal amounts of cell extract protein were blotted against p-ezrin and ezrin utilizing specific antibodies. (C) Protein bands were densitometrically analyzed and adjusted against actin. The results represent the average of three separate experiments in triplicate. Means ± S.E.M plotted; Statistical significance *p ≤ 0.05, ** p ≤ 0.01, among samples.

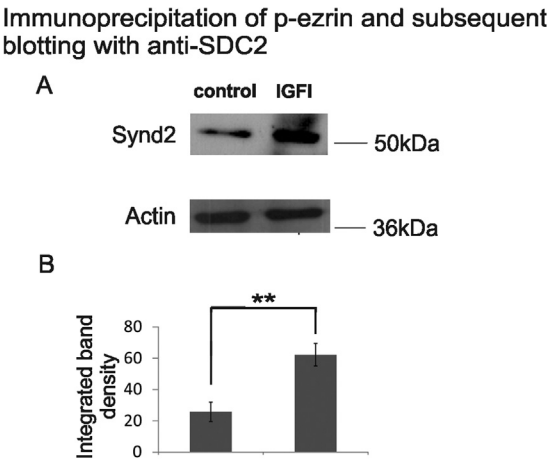

Fig. 5. Co-immunoprecipitation of SDC2 and p-ezrin. (A) HT1080 cells were treated with DMEM 0%, or with IGFI (5 ng/ml) for 1 h or 24 h, whereupon they were harvested and cell extract proteins obtained. Western blot analysis was used for the visualization of ezrin protein expression in control cells treated with culture medium (control), samples treated with IGF-I and immunoprecipitated with anti-SDC-2 in the cell extracts stored from each sample (total protein) of the same experiment. B. Densitometric analysis of the bands was normalized against actin and plotted. The results represent the average of three separate experiments. Means ± S.E.M. plotted; statistical significance is as follows: **p ≤ 0.001 compared with the respective control samples.

regulation by IGF-I signaling we used immunoflorescence. After treatment of HT1080 cells with IGF-I and special permeabilization procedure, staining with SDC2 (green signal) and ezrin (red signal) antibodies was performed. The co-localization was identified after signal superimposition (orange signal) with a significant enhancement of the superimposed signal in IGFI-treated cells (Fig. 6).

In continuation, the HT1080 cells were stained for SDC2, IGF-IR and TO-PRO-3 (nuclear staining). The resulting yellow/orange staining of the antibody signals, verified the existence of an association among SDC2 and IFG-IR. Likewise, the superimposed signal was more pronounced in IGF-I -treated HT1080 cells when compared with control (Fig. 7). These results suggest a close association among IGF-IR, SDC-2 and ezrin in a manner dependent on IGF-I.

3.6. Ezrin and phalloidin co-localize in HT1080 cells in a manner dependent on IGF-I signaling

Ezrin is known to be a membrane-cytoskeleton-linker protein [54]. To examine the possible IGF-I mediated association between ezrin and actin in our model system we used immunofluorescence. HT1080 cells were treated with IGF-I and stained against p-ezrin, actin and TO-PRO-3. *Cells treated with IGF-I exhibited a stronger staining for phaloidin (red color) as well as pronounced ezrin/actin co-localization (superimposed yellow/orange staining) detected mostly at the cell membranes* (Fig. 8). *Thus, our results suggest that IGF-I enhances actin filament organization and their cell membrane linking through specific p-ezrin/actin membrane co-localization* (Fig. 8).

3.7. IGFI modulates SDC2 mRNA and protein expression

IGF-I has been shown to affect syndecan expression in a cell type dependent manner [58]. In order to further investigate the contribution of SDC2 on IFG-I-dependent migration we examined the effects of IGF-I on SDC2 expression. Real-time PCR demonstrated that HT1080 cells treated with IGF-I for 24 h, expressed significantly higher levels of SDC2 mRNA as compared to control ($p < 0.001$) (Fig. 9A) whereas, western blotting, showed that treatment with IGF-I resulted in a strong increase in SDC2 protein expression in HT1080 cells, as compared to control ($p < 0.001$) (Fig. 9B and C) ($p < 0.001$). Further evidence for SDC2 expression modulation by IGF-I was provided using immunofluorescence, where IGF-I increased total specific SDC2 signal (Fig. 9D).

4. Discussion

The ability of SDC2 to control cell signaling is now well associated with the regulation of cell behaviour and especially cancer progression [59]. This transmembrane proteoglycan, which is highly expressed in mesenchymal cells, was previously shown to enhance fibrosarcoma cell migration through a FAK/PI3K/Tiam1/Rac-dependent axis [38]. Importantly, Klass et al., demonstrated that Chinese Hamster Ovary (CHO) cells stably transfected with truncated SDC-2, which lacks the C-terminal 14 amino acids of the cytoplasmic domain (S2deltaS) lost the ability to rearrange laminin or FN substrates into fibrils and to bind exogenous FN [60]. Moreover, Peterfia et al., revealed its collaboration with SDC1 in the induction of HT1080 cell proliferation and chemotaxis [41]. Interestingly, in the same study, SDC2 synthesis was suggested to be controlled by IGF-IR in fibosarcoma [41], a connection which was later confirmed in breast cancer [59].

The strong oncogenic profile of IGF-I is well established in the literature [12,15,19]. IGF-I is implicated in the regulation of apoptosis, angiogenesis and metastasis and it is able to promote cancer progression through its receptor IGF-IR [12,61], which is highly expressed on the cell surface of HT1080 cells [62]. The role of IGF-I as a potent promoter of fibrosarcoma cell metastasis has already been highlighted in previous studies [19,63].

The main downstream signaling pathways of IGF-I include the

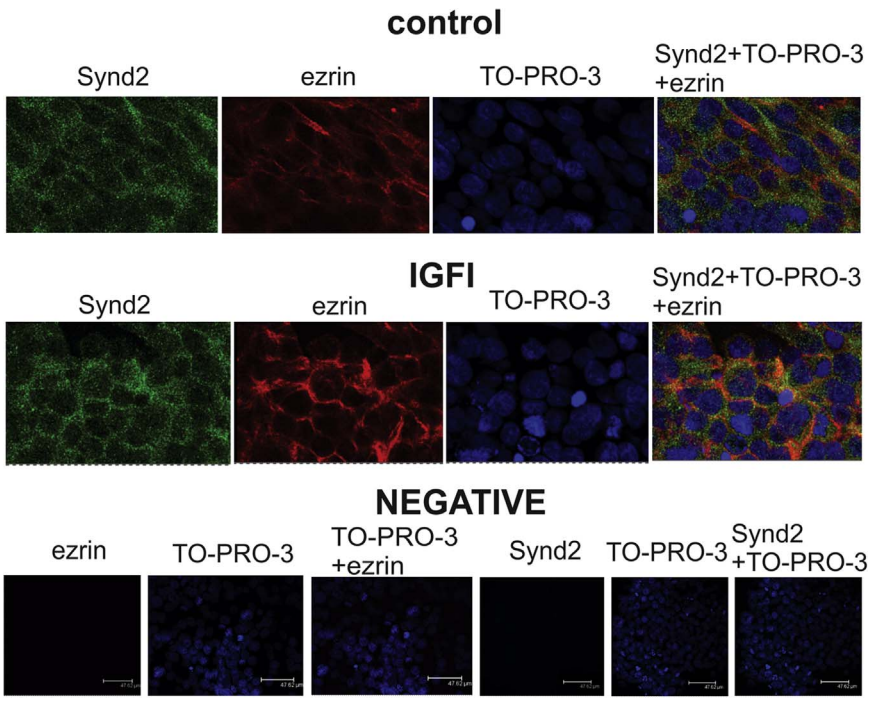

Fig. 6. Visualization of SDC2 and ezrin co-localization in HT1080 cells with immunofluorescence. HT1080 cells were treated with DMEM 0%, or IGFI (5 ng/ml) and after 24 h incubation, cells were fixed, permeabilized on coverslips and stained for SDC2 and ezrin specific antibodies along with the respective nuclei, using TO-PRO-3. Negative controls did not contain SDC2 and ezrin antibodies. Signals against SDC2 (green) and ezrin (red) were superimposed (yellow-orange signal). Slides were analyzed by confocal microscopy and pictures were taken using × 40 (with × 10 zoom) magnification.

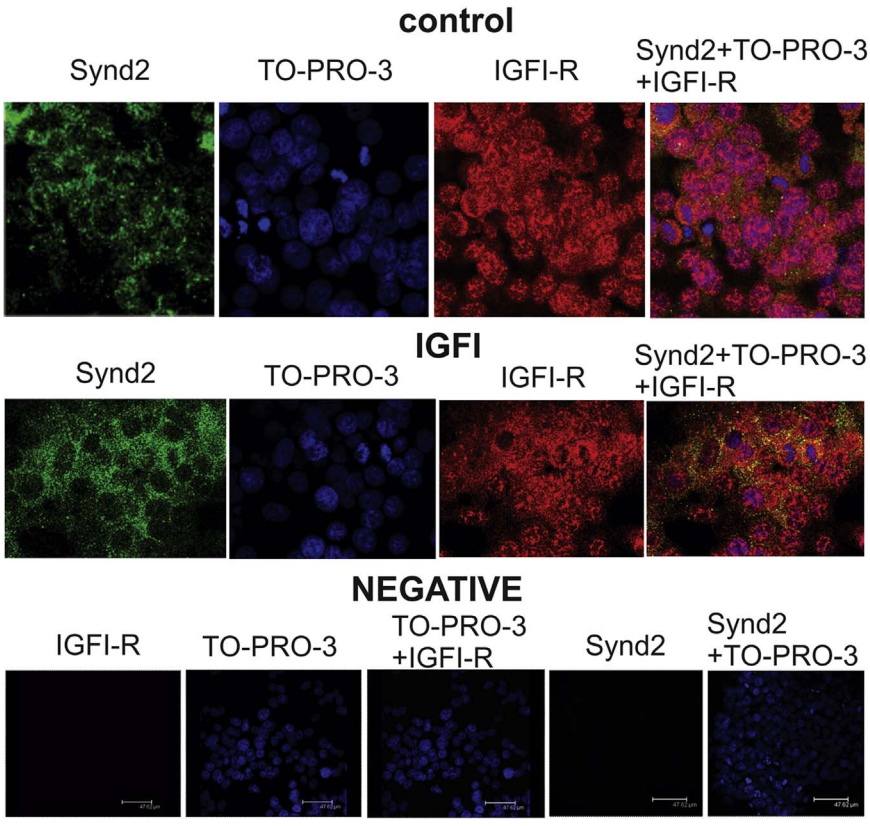

Fig. 7. Visualization of SDC2 and IGFI-R co-localization in HT1080 cells. HT1080 cells were cultured in DMEM 0%, or IGFI (5 ng/ml) and then, they were seeded onto round coverslips, they were fixed, permeabilized, and stained using SDC2 (green signal) and IGFI-R (red signal) specific antibodies. Nuclei were stained with TO-PRO-3. In negative controls, the primary anti-SDC2 and anti-IGFI-R were omitted. Slides were analyzed by confocal microscopy, and pictures were taken using × 40 (with × 10 zoom) magnification.

phosphorylation of ERK1/2 and AKT [28,64]. It seems that SDC2 participates in the regulation of IGF-I downstream signaling, as it can control ERK phosphorylation in sarcomas [41,65]. Noteworthy, IGF-I pathway is one of major intracellular mediators of proliferation and motility [28]. Furthermore, it has been suggested that SDC2 and IGF-IR form a feedback loop together, as IGF-IR is found to induce SDC2 expression [59]; whereas conversely, SDC2 can down-regulate IGF-IR expression [41]. Taking these data into account, we found it interesting to delineate the convergence of these pathways during fibrosarcoma cells' chemotactic migration and examine a potential topological

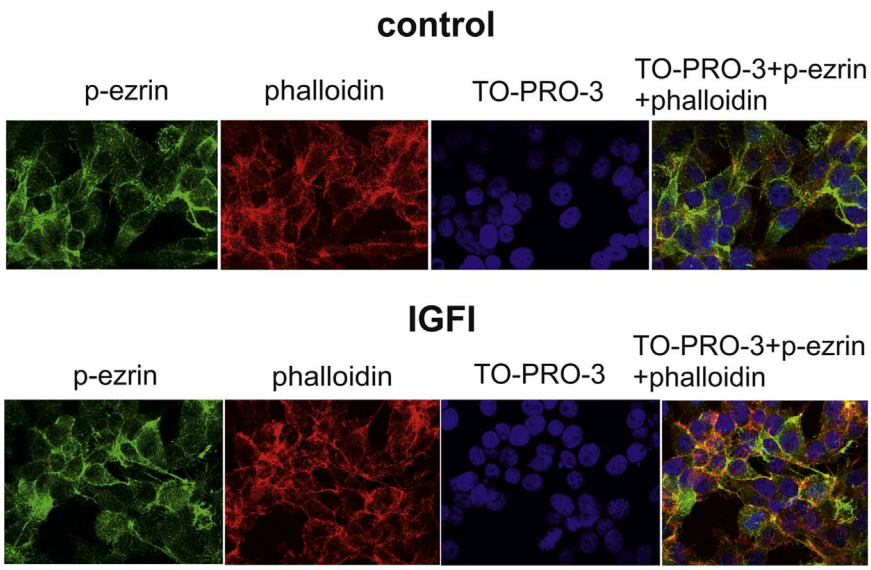

Fig. 8. IGF-I signaling regulates actin cytoskeleton organization. HT1080 cells were either treated with DMEM 0%, or IGFI (5 ng/ml) for 24 h. Afterwards, they were seeded onto round coverslips and stained against p-ezrin (green signal) and phalloidin (red signal) to visualize actin filaments' formation. The nuclei were stained with TO-PRO 3. The signals against actin filaments and p-ezrin were superimposed (yellow signal). In the negative controls, anti-p-ezrin and anti-phalloidin were omitted. Slides were analyzed by confocal microscopy and pictures were taken using × 40 (with × 10 zoom) magnification.

affinity of SDC2 and IGF-IR.

We demonstrate for the first time that IGFI/IGFIR enhance the chemotactic motility of HT1080 cells through a SDC2-dependent mechanism. In a previous study on human multiple myeloma cells, IGF-I was shown to activate IGF-IR, which triggered the polymerization of F-actin, induced phosphorylation of p125(FAK) and paxillin, and enhanced interactions of these focal adhesion proteins with beta1 integrin to facilitate FN-dependent adhesion [64]. In the present study and in line with previous publications about the tumorigenic effects of ERK1/2 [28,66–68], we show that IGF-IR-dependent activation of Erk1/2 plays a crucial role in the execution of IGF-I-mediated *HT1080* fibrosarcoma cell migration. Moreover, we demonstrate that silencing of SDC2 attenuates IGFI-induced ERK1/2 phosphorylation and subsequently eliminates one of IGF-I main signal transducers and tumor progression mediators. *B6FS fibrosarcoma cells' motility was not responsive to IGF-I modulation. B6FS cell line originates from a poorly differentiated fibrosarcoma* [43]*, where the cells are characterized by scant phenotypic similarity with cells of origin, mild pleomorphism, as well as intense mitotic activity* [69,70]*. Moreover, SDC2 did not affect B6FS cell migration. This is in accordance with a previous study demonstrating that B6FS cells' adhesion was not sensitive to their heparan sulfate glycosylation pattern* (45)*. The differences in the two fibrosarcoma cell lines responses to IGF-I/SDC2 signaling can be attributed to fibrosarcoma heterogeneity as regarding morphology, differentiation and behaviour* [71]*. Noteworthy, even though the emerging evidence introduces a strong cancer-promoting role for SDC2 in majority of epithelial tumors; mesenchymal type tumors exhibit a more specific tumor-type response* [39,41,72].

Taking into account the unique properties of SDC2, we attempted to expand our understanding on its regulatory role in the motility of HT1080 fibrosarcoma cells [5]. In order to clarify the correlation between SDC2 and IGF-IR signaling we examined their respective localization on cell membrane utilizing immunoprecipitation and immunofluorescence assays. This approach demonstrated that IGF-IR is co-localized with SDC2 in fibrosarcoma and this co-localization is up-regulated in the presence of IGFI. In light of the previously mentioned data, we hypothesize that SDC2 acts synergistically with IGF-IR at the cell membrane, which subsequently results in upregulation of IGF-IR downstream signaling. Furthermore, it is well established that SDC2 is responsible for the reorganization of actin cytoskeleton [38], forming filopodia and ultimately affecting cell motility [54,73,74]. Through these properties, SDC2 is able to transmit extracellular matrix cues into the cell and affect cell behaviour [54,75]. Moreover, a direct association between the N-terminal domain of ezrin and the cytoplasmic domain of SDC2 was previously indicated [54]. Ezrin being a cytoplasmic protein was suggested to act as a signaling bridge between the cellular membrane receptors and actin cytoskeleton [54]. Indeed, even early reports indicate that activated ezrin monomers or head-to-tail oligomers associate directly with F-actin through a domain in its C terminus, and with the membrane through its N-terminal domain [76]. Furthermore, it is widely accepted that ezrin, radixin and moesin (ERM) proteins exist in an apparently dormant, closed conformation that localizes in the cytoplasm and only upon activation are able to interact with plasma membrane proteins and actin filaments [77]. Thus, it is the phosporylation at Thr-567 that is sufficient to disrupt the closed conformation of ezrin and transform it into the active form, which is able to bind F-actin [78]. Ezrin has previously been shown to be activated by IGF-I at lamellipodia of ovarian and cervical cancer cells where its' subsequent co-localization with the KCl cotransporter-4 facilitates cancer cell invasion [79]. Moreover, in astroglia cells, ezrin has been designated the role of a coordinator of actin linking to the membrane, through IGF-IR auto-phosphorylation upon ligand binding [80].

Results of this study confirm these functional roles of ezrin in fibrosarcoma, as IGFI-treated cells exhibit enhanced ezrin activation and increased SDC2-ezrin co-localization. IGFI/IGFIR seem to be crucial for these interactions, since our findings show that IGF-IR activation affects directly the phosphorylation of ezrin and SDC2-ezrin co-localization. *The phosphorylation of ezrin resulted in the amplification of ezrin/actin complexes. Complex localization was most prominent to the cell membranes suggesting that ezrin coordinates the linking of actin filaments to membrane superstructure as previously shown in other models* [80]. On the other hand, ezrin has also been previously found to control the phosphorylation of ERK1/2, downstream of EGFR in non-small cell lung cancer cells [81]. These data suggest that both SDC2 and ezrin are potential ERK1/2 activators. Thus, apart from the direct roles of SDC2/ezrin in *actin filament organization*, these mediators might also amplify fibrosarcoma migration indirectly, either through ERK1/2-induced expression of cancer-related proteins, or through ERK1/2-related changes in actin morphology, according to a recent finding in glioblastoma cells [82]. Interestingly our study suggests an existence of a feedback loop supported by the identified increase of SDC2 expression in fibrosarcoma cells treated with IGF-I. Therefore, SDC2 stabilizes the IFG-IR receptor, facilitates its downstream signaling propagating a vicious loop that

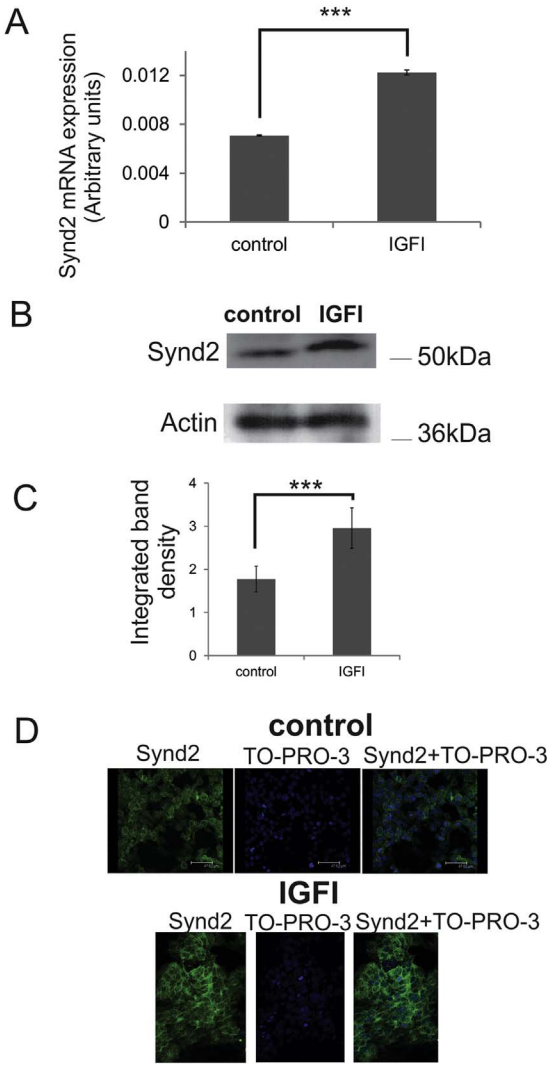

Fig. 9. IGF-I modulates SDC2 mRNA and protein expression. (A) Expression of SDC2 was quantified by Real-time PCR, after treatment either with DMEM 0%, or IGFI (5 ng/ml) for 24 h. The results represent the average of three separate experiments in triplicate. Means ± S.E.M plotted; Statistical significance ***p ≤ 0.001 among control and respective treatments. B: HT1080 cells were either treated with DMEM 0%, or with IGFI (5 ng/ml) for 24 h. After harvesting, equal amounts of cell extract proteins were blotted against SDC2 specific antibody. Representative blots are presented. Specific SDC2 protein bands were densitometrically analyzed and adjusted against actin. The results represent the average of three separate experiments in triplicate. Means ± S.E.M plotted; Statistical significance ***p ≤ 0.001 among control and respective treatments. (C) SDC2 protein staining of cells (green signal) and respective nuclear staining (using TO-PRO-3) (blue signal) were evaluated in cultures after 24 h incubation with DMEM 0% and IGFI (5 ng/ml). A negative control was used, where the primary anti-SDC2 antibody was omitted (negative). Slides were analyzed by confocal microscopy, and pictures were taken using × 40 (with × 10 zoom) magnification.

enhances the motile behaviour of the HT1080 cells. The suggested SDC2/IGF-IR, ERK1,2/ezrin axis regulating actin organization and HT1080 fibrosarcoma migration is presented in Fig. 10.

In conclusion, we propose a novel SDC2-dependent strategy, where SDC2 is co-localized with IGF-IR, stabilizes the receptor and enhances its IGFI-dependent downstream signaling. SDC2 mediates IGF-IR-induced ezrin activation and recruitment, *contributes to actin filament organization ultimately facilitating the progression of IGFI-dependent HT1080 fibrosarcoma cell migration.* In parallel, SDC2 facilitates IGF-IR –dependent ERK1/2 activation and resulting target gene among other SDC2 transcription, which results in increased SDC2 expression and amplification of the signaling circuit. *No effect of SDC2 was established on B6FS cells' migration. This finding however, is well in accord with discrete effect of*

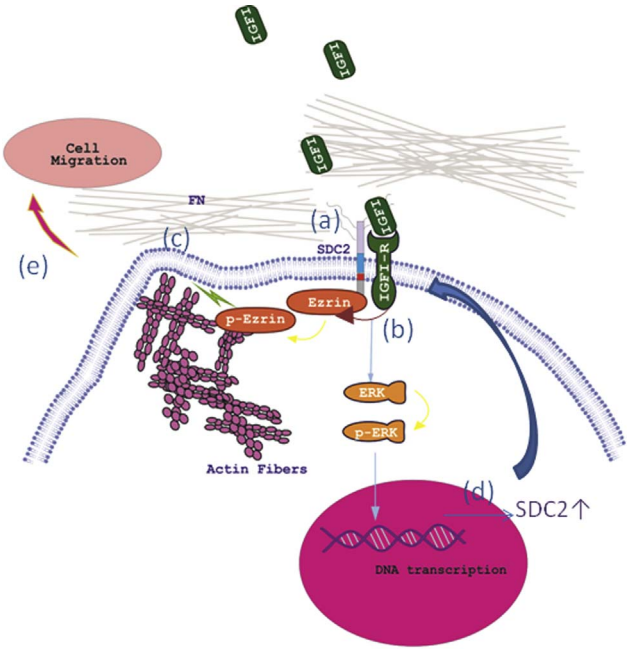

Fig. 10. SDC2 regulates IGF-IR signaling. (A) SDC2 co-localizes with IGF-IR, stabilizes the receptor and enhances its downstream signaling. (B) IGF-IR phosphorylates ezrin activating it and allowing its co-localization with SDC2 (C) Ezrin initiates actin fiber organization and formation of filopodia (D) IGF-IR and/or ezrin phosphorylate ERK1/2 resulting in transcription of target genes including increase in SDC2 expression, amplifying the signaling circuit and (E) resulting FS migration.

SDC2 on mesenchymal origin tumors. Further studies are needed to clarify the functional relationship of SDC2 with IGF-IR and the circuit involved in IGF-I signaling, which may be useful in the design of a more effective, molecule-oriented treatment for human fibrosarcoma.

Appendix A. Supplementary material

Supplementary data associated with this article can be found in the online version at http://dx.doi.org/10.1016/j.yexcr.2017.09.035.

References

[1] A. Franchi, M. Santucci, The contribution of electron microscopy to the characterization of soft tissue fibrosarcomas, Ultrastruct. Pathol. 37 (2013) 9–14.
[2] A. Bahrami, A.L. Folpe, Adult-type fibrosarcoma: a reevaluation of 163 putative cases diagnosed at a single institution over a 48-year period, Am. J. Surg. Pathol. 34 (2010) 1504–1513.
[3] P.J. Papagelopoulos, E.C. Galanis, P. Trantafyllidis, P.J. Boscainos, F.H. Sim, K.K. Unni, Clinicopathologic features, diagnosis, and treatment of fibrosarcoma of bone, Am. J. Orthop. 31 (2002) 253–257.
[4] V. Wadhwan, M.S. Chaudhary, M. Gawande, Fibrosarcoma of the oral cavity, Indian J. Dent. Res.: Off. Publ. Indian Soc. Dent. Res. 21 (2010) 295–298.
[5] M. Mytilinaiou, A. Bano, D. Nikitovic, A. Berdiaki, K. Voudouri, A. Kalogeraki, N.K. Karamanos, G.N. Tzanakakis, Syndecan-2 is a key regulator of transforming growth factor beta 2/Smad2-mediated adhesion in fibrosarcoma cells, IUBMB life 65 (2013) 134–143.
[6] A. Fiorelli, C. Ricciardi, G. Pannone, A. Santoro, P. Bufo, M. Santini, R. Serpico, R. Rullo, G.M. Pierantoni, M. Di Domenico, Interplay between steroid receptors and neoplastic progression in sarcoma tumors, J. Cell. Physiol. 226 (2011) 2997–3003.
[7] Y.P. Hwang, H.J. Yun, J.H. Choi, E.H. Han, H.G. Kim, G.Y. Song, K.I. Kwon, T.C. Jeong, H.G. Jeong, Suppression of EGF-induced tumor cell migration and matrix metalloproteinase-9 expression by capsaicin via the inhibition of EGFR-mediated FAK/Akt, PKC/Raf/ERK, p38 MAPK, and AP-1 signaling, Mol. Nutr. Food Res. 55 (2011) 594–605.
[8] E. Fthenou, A. Zafiropoulos, A. Tsatsakis, A. Stathopoulos, N.K. Karamanos, G.N. Tzanakakis, Chondroitin sulfate A chains enhance platelet derived growth factor-mediated signalling in fibrosarcoma cells, Int. J. Biochem. Cell Biol. 38 (2006) 2141–2150.
[9] D. Nikitovic, A. Berdiaki, A. Banos, A. Tsatsakis, N.K. Karamanos, G.N. Tzanakakis, Could growth factor-mediated extracellular matrix deposition and degradation offer the ground for directed pharmacological targeting in fibrosarcoma? Curr. Med. Chem. 20 (2013) 2868–2880.
[10] R.H. Nielsen, L. Holm, N.M. Malmgaard-Clausen, S. Reitelseder, K.M. Heinemeier,

M. Kjaer, Increase in tendon protein synthesis in response to insulin-like growth factor-I is preserved in elderly men, J. Appl. Physiol. 116 (2014) 42–46.
[11] K.L. Hull, S. Harvey, Growth hormone and reproduction: a review of endocrine and autocrine/paracrine interactions, Int. J. Endocrinol. 2014 (2014) 234014.
[12] V.P. Brahmkhatri, C. Prasanna, H.S. Atreya, Insulin-like growth factor system in cancer: novel targeted therapies, BioMed. Res. Int. 2015 (2015) 538019.
[13] E.J. Gallagher, D. LeRoith, Minireview: IGF, insulin, and cancer, Endocrinology 152 (2011) 2546–2551.
[14] R.G. Maki, Small is beautiful: insulin-like growth factors and their role in growth, development, and cancer, J. Clin. Oncol.: Off. J. Am. Soc. Clin. Oncol. 28 (2010) 4985–4995.
[15] A.A. Samani, S. Yakar, D. LeRoith, P. Brodt, The role of the IGF system in cancer growth and metastasis: overview and recent insights, Endocr. Rev. 28 (2007) 20–47.
[16] N.J. Balamuth, R.B. Womer, Ewing's sarcoma, Lancet Oncol. 11 (2010) 184–192.
[17] G. Furstenberger, H.J. Senn, Insulin-like growth factors and cancer, Lancet Oncol. 3 (2002) 298–302.
[18] D. LeRoith, C.T. Roberts Jr., The insulin-like growth factor system and cancer, Cancer Lett. 195 (2003) 127–137.
[19] A. Sekyi-Otu, R. Bell, I. Andrulis, M. Pollak, Metastatic behavior of the RIF-1 murine fibrosarcoma: inhibited by hypophysectomy and partially restored by growth hormone replacement, J. Natl. Cancer Inst. 86 (1994) 628–632.
[20] H.A. Zielinska, A. Bahl, J.M. Holly, C.M. Perks, Epithelial-to-mesenchymal transition in breast cancer: a role for insulin-like growth factor I and insulin-like growth factor-binding protein 3? Breast Cancer 7 (2015) 9–19.
[21] P.V. Peplow, M.P. Chatterjee, A review of the influence of growth factors and cytokines in in vitro human keratinocyte migration, Cytokine 62 (2013) 1–21.
[22] Q. Zhou, J. Zhang, Q. Cui, X. Li, G. Gao, Y. Wang, Y. Xu, X. Gao, GSK1904529A, an insulin-like growth factor-1 receptor inhibitor, inhibits glioma tumor growth, induces apoptosis and inhibits migration, Mol. Med. Rep. 12 (2015) 3381–3385.
[23] L. Bieghs, H.E. Johnsen, K. Maes, E. Menu, E. Van Valckenborgh, M.T. Overgaard, M. Nyegaard, C.A. Conover, K. Vanderkerken, E. De Bruyne, The insulin-like growth factor system in multiple myeloma: diagnostic and therapeutic potential, Oncotarget 7 (2016) 48732–48752.
[24] N. Armakolas, A. Armakolas, A. Antonopoulos, A. Dimakakos, M. Stathaki, M. Koutsilieris, The role of the IGF-1 Ec in myoskeletal system and osteosarcoma pathophysiology, Crit. Rev. Oncol./Hematol. 108 (2016) 137–145.
[25] F. Li, H. Wang, L. Li, C. Huang, J. Lin, G. Zhu, Z. Chen, N. Wu, H. Feng, Superoxide plays critical roles in electrotaxis of fibrosarcoma cells via activation of ERK and reorganization of the cytoskeleton, free radical biology & medicine, 52 (2012) 1888–1896.
[26] H. Nam, M.M. Kim, Eugenol with antioxidant activity inhibits MMP-9 related to metastasis in human fibrosarcoma cells, Food Chem. Toxicol.: Int. J. Publ. Br. Ind. Biol. Res. Assoc. 55 (2013) 106–112.
[27] K.C. Williams, M.G. Coppolino, Phosphorylation of membrane type 1-matrix metalloproteinase (MT1-MMP) and its vesicle-associated membrane protein 7 (VAMP7)-dependent trafficking facilitate cell invasion and migration, J. Biol. Chem. 286 (2011) 43405–43416.
[28] R. Subramani, R. Lopez-Valdez, A. Arumugam, S. Nandy, T. Boopalan, R. Lakshmanaswamy, Targeting insulin-like growth factor 1 receptor inhibits pancreatic cancer growth and metastasis, PloS One 9 (2014) e97016.
[29] S.S. Skandalis, N. Afratis, G. Smirlaki, D. Nikitovic, A.D. Theocharis, G.N. Tzanakakis, N.K. Karamanos, Cross-talk between estradiol receptor and EGFR/IGF-IR signaling pathways in estrogen-responsive breast cancers: focus on the role and impact of proteoglycans, Matrix Biol.: J. Int. Soc. Matrix Biol. 35 (2014) 182–193.
[30] K. Voudouri, D. Nikitovic, A. Berdiaki, D. Kletsas, N.K. Karamanos, G.N. Tzanakakis, IGF-I/EGF and E2 signaling crosstalk through IGF-IR conduit point affects breast cancer cell adhesion, Matrix Biol.: J. Int. Soc. Matrix Biol. 56 (2016) 95–113.
[31] E.A. Kolb, R. Gorlick, Development of IGF-IR Inhibitors in Pediatric Sarcomas, Curr. Oncol. Rep. 11 (2009) 307–313.
[32] D. Olmos, S. Postel-Vinay, L.R. Molife, S.H. Okuno, S.M. Schuetze, M.L. Paccagnella, G.N. Batzel, D. Yin, K. Pritchard-Jones, I. Judson, F.P. Worden, A. Gualberto, M. Scurr, J.S. de Bono, P. Haluska, Safety, pharmacokinetics, and preliminary activity of the anti-IGF-1R antibody figitumumab (CP-751,871) in patients with sarcoma and Ewing's sarcoma: a phase 1 expansion cohort study, Lancet Oncol. 11 (2010) 129–135.
[33] K. Scotlandi, M.C. Manara, G. Nicoletti, P.L. Lollini, S. Lukas, S. Benini, S. Croci, S. Perdichizzi, D. Zambelli, M. Serra, C. Garcia-Echeverria, F. Hofmann, P. Picci, Antitumor activity of the insulin-like growth factor-I receptor kinase inhibitor NVP-AEW541 in musculoskeletal tumors, Cancer Res. 65 (2005) 3868–3876.
[34] Z. Wang, D. Telci, M. Griffin, Importance of syndecan-4 and syndecan −2 in osteoblast cell adhesion and survival mediated by a tissue transglutaminase-fibronectin complex, Exp. Cell Res. 317 (2011) 367–381.
[35] S. Gopal, J. Couchman, R. Pocock, Redefining the role of syndecans in C. elegans biology, Worm 5 (2016) e1142042.
[36] K. Vuoriluoto, J. Jokinen, K. Kallio, M. Salmivirta, J. Heino, J. Ivaska, Syndecan-1 supports integrin alpha2beta1-mediated adhesion to collagen, Exp. Cell Res. 314 (2008) 3369–3381.
[37] N.A. Afratis, D. Nikitovic, H.A. Multhaupt, A.D. Theocharis, J.R. Couchman, N.K. Karamanos, Syndecans - key regulators of cell signaling and biological functions, FEBS J. 284 (2017) 27–41.
[38] H. Park, I. Han, H.J. Kwon, E.S. Oh, Focal adhesion kinase regulates syndecan-2-mediated tumorigenic activity of HT1080 fibrosarcoma cells, Cancer Res. 65 (2005) 9899–9905.
[39] A. Orosco, O. Fromigue, C. Bazille, N. Entz-Werle, P. Levillain, P.J. Marie, D. Modrowski, Syndecan-2 affects the basal and chemotherapy-induced apoptosis in osteosarcoma, Cancer Res. 67 (2007) 3708–3715.
[40] J.R. Whiteford, V. Behrends, H. Kirby, M. Kusche-Gullberg, T. Muramatsu, J.R. Couchman, Syndecans promote integrin-mediated adhesion of mesenchymal cells in two distinct pathways, Exp. Cell Res. 313 (2007) 3902–3913.
[41] B. Peterfia, T. Fule, K. Baghy, K. Szabadkai, A. Fullar, K. Dobos, F. Zong, K. Dobra, P. Hollosi, A. Jeney, S. Paku, I. Kovalszky, Syndecan-1 enhances proliferation, migration and metastasis of HT-1080 cells in cooperation with syndecan-2, PloS One 7 (2012) e39474.
[42] S. Rasheed, W.A. Nelson-Rees, E.M. Toth, P. Arnstein, M.B. Gardner, Characterization of a newly derived human sarcoma cell line (HT-1080), Cancer 33 (1974) 1027–1033.
[43] V. Thurzo, M. Popovic, J. Matoska, M. Blasko, M. Grofova, A. Lizonova, M. Steno, Human neoplastic cells in tissue culture: two established cell lines derived from giant cell tumor and fibrosarcoma, Neoplasma 23 (1976) 577–587.
[44] K. Kouvidi, A. Berdiaki, M. Tzardi, E. Karousou, A. Passi, D. Nikitovic, G.N. Tzanakakis, Receptor for hyaluronic acid- mediated motility (RHAMM) regulates HT1080 fibrosarcoma cell proliferation via a beta-catenin/c-myc signaling axis, Biochim. Et. Biophys. Acta 1860 (2016) 814–824.
[45] K. Voudouri, D. Nikitovic, A. Berdiaki, D.J. Papachristou, J. Tsiaoussis, D.A. Spandidos, A.M. Tsatsakis, G.N. Tzanakakis, Heparin regulates B6FS cell motility through a FAK/actin cytoskeleton axis, Oncol. Rep. 36 (2016) 2471–2480.
[46] G. Chalkiadaki, D. Nikitovic, A. Berdiaki, P. Katonis, N.K. Karamanos, G.N. Tzanakakis, Heparin plays a key regulatory role via a p53/FAK-dependent signaling in melanoma cell adhesion and migration, IUBMB life 63 (2011) 109–119.
[47] G. Chalkiadaki, D. Nikitovic, P. Katonis, A. Berdiaki, A. Tsatsakis, I. Kotsikogianni, N.K. Karamanos, G.N. Tzanakakis, Low molecular weight heparin inhibits melanoma cell adhesion and migration through a PKCa/JNK signaling pathway inducing actin cytoskeleton changes, Cancer Lett. 312 (2011) 235–244.
[48] M.M. Chitnis, J.S. Yuen, A.S. Protheroe, M. Pollak, V.M. Macaulay, The type 1 insulin-like growth factor receptor pathway, Clin. Cancer Res.: Off. J. Am. Assoc. Cancer Res. 14 (2008) 6364–6370.
[49] W. Jeong, G. Song, F.W. Bazer, J. Kim, Insulin-like growth factor I induces proliferation and migration of porcine trophectoderm cells through multiple cell signaling pathways, including protooncogenic protein kinase 1 and mitogen-activated protein kinase, Mol. Cell. Endocrinol. 384 (2014) 175–184.
[50] C. Duan, The chemotactic and mitogenic responses of vascular smooth muscle cells to insulin-like growth factor-I require the activation of ERK1/2, Mol. Cell. Endocrinol. 206 (2003) 75–83.
[51] H. Li, L. Xu, C. Li, L. Zhao, Y. Ma, H. Zheng, Z. Li, Y. Zhang, R. Wang, Y. Liu, X. Qu, Ubiquitin ligase Cbl-b represses IGF-I-induced epithelial mesenchymal transition via ZEB2 and microRNA-200c regulation in gastric cancer cells, Mol. Cancer 13 (2014) 136.
[52] A. Armakolas, M. Kaparelou, A. Dimakakos, E. Papageorgiou, N. Armakolas, A. Antonopoulos, C. Petraki, M. Lekarakou, P. Lelovas, M. Stathaki, C. Psarros, I. Donta, P.S. Galanos, P. Msaouel, V.G. Gorgoulis, M. Koutsilieris, Oncogenic role of the Ec peptide of the IGF-1Ec isoform in prostate cancer, Mol. Med. 21 (2015) 167–179.
[53] F. Granes, C. Berndt, C. Roy, P. Mangeat, M. Reina, S. Vilaro, Identification of a novel Ezrin-binding site in syndecan-2 cytoplasmic domain, FEBS Lett. 547 (2003) 212–216.
[54] F. Granes, J.M. Urena, N. Rocamora, S. Vilaro, Ezrin links syndecan-2 to the cytoskeleton, J. Cell Sci. 113 (Pt 7) (2000) 1267–1276.
[55] F. Tang, D. Wang, C. Duan, D. Huang, Y. Wu, Y. Chen, W. Wang, C. Xie, J. Meng, L. Wang, B. Wu, S. Liu, D. Tian, F. Zhu, Z. He, F. Deng, Y. Cao, Berberine inhibits metastasis of nasopharyngeal carcinoma 5–8F cells by targeting Rho kinase-mediated Ezrin phosphorylation at threonine 567, J. Biol. Chem. 284 (2009) 27456–27466.
[56] R.G. Fehon, A.I. McClatchey, A. Bretscher, Organizing the cell cortex: the role of ERM proteins, Nat. Rev. Mol. Cell Biol. 11 (2010) 276–287.
[57] P.D. Leiphrakpam, A. Rajput, M. Mathiesen, E. Agarwal, A.J. Lazenby, C. Are, M.G. Brattain, S. Chowdhury, Ezrin expression and cell survival regulation in colorectal cancer, Cell. Signal. 26 (2014) 868–879.
[58] K. Dobra, M. Nurminen, A. Hjerpe, Growth factors regulate the expression profile of their syndecan co-receptors and the differentiation of mesothelioma cells, Anticancer Res. 23 (2003) 2435–2444.
[59] A.I. Tsonis, N. Afratis, C. Gialeli, M.I. Ellina, Z. Piperigkou, S.S. Skandalis, A.D. Theocharis, G.N. Tzanakakis, N.K. Karamanos, Evaluation of the coordinated actions of estrogen receptors with epidermal growth factor receptor and insulin-like growth factor receptor in the expression of cell surface heparan sulfate proteoglycans and cell motility in breast cancer cells, FEBS J. 280 (2013) 2248–2259.
[60] C.M. Klass, J.R. Couchman, A. Woods, Control of extracellular matrix assembly by syndecan-2 proteoglycan, J. Cell Sci. 113 (Pt 3) (2000) 493–506.
[61] T. Takahashi, H. Uehara, H. Ogawa, H. Umemoto, Y. Bando, K. Izumi, Inhibition of EP2/EP4 signaling abrogates IGF-1R-mediated cancer cell growth: involvement of protein kinase C-theta activation, Oncotarget 6 (2015) 4829–4844.
[62] X. Huang, H. Park, J. Greene, J. Pao, E. Mulvey, S.X. Zhou, C.M. Albert, F. Moy, D. Sachdev, D. Yee, C. Rader, C.V. Hamby, D.M. Loeb, M.S. Cairo, X. Zhou, IGF1R- and ROR1-Specific CAR T Cells as a Potential Therapy for High Risk Sarcomas, PloS One 10 (2015) e0133152.
[63] A. Yoon, R.A. Hurta, Insulin like growth factor-1 selectively regulates the expression of matrix metalloproteinase-2 in malignant H-ras transformed cells, Mol. Cell. Biochem. 223 (2001) 1–6.
[64] Y.T. Tai, K. Podar, L. Catley, Y.H. Tseng, M. Akiyama, R. Shringarpure, R. Burger, T. Hideshima, D. Chauhan, N. Mitsiades, P. Richardson, N.C. Munshi, C.R. Kahn, C. Mitsiades, K.C. Anderson, Insulin-like growth factor-1 induces adhesion and

migration in human multiple myeloma cells via activation of beta1-integrin and phosphatidylinositol 3′-kinase/AKT signaling, Cancer Res. 63 (2003) 5850–5858.
[65] D. Modrowski, A. Orosco, J. Thevenard, O. Fromigue, P.J. Marie, Syndecan-2 overexpression induces osteosarcoma cell apoptosis: implication of syndecan-2 cytoplasmic domain and JNK signaling, Bone 37 (2005) 180–189.
[66] Y. Matsunaga, Y. Adachi, Y. Sasaki, H. Koide, M. Motoya, K. Nosho, H. Takagi, H. Yamamoto, S. Sasaki, Y. Arimura, T. Tokino, D.P. Carbone, K. Imai, Y. Shinomura, The effect of forced expression of mutated K-RAS gene on gastrointestinal cancer cell lines and the IGF-1R targeting therapy, Mol. Carcinog. 56 (2017) 515–526.
[67] M. Meister, A. Tomasovic, A. Banning, R. Tikkanen, Mitogen-activated protein (MAP) kinase scaffolding proteins: a recount, Int. J. Mol. Sci. 14 (2013) 4854–4884.
[68] H. Chen, G. Zhu, Y. Li, R.N. Padia, Z. Dong, Z.K. Pan, K. Liu, S. Huang, Extracellular signal-regulated kinase signaling pathway regulates breast cancer cell migration by maintaining slug expression, Cancer Res. 69 (2009) 9228–9235.
[69] K. Thway, D. Robertson, R.L. Jones, J. Selfe, J. Shipley, C. Fisher, C.M. Isacke, Endosialin expression in soft tissue sarcoma as a potential marker of undifferentiated mesenchymal cells, Br. J. Cancer 115 (2016) 473–479.
[70] J. Noujaim, K. Thway, A. Sheri, C. Keller, R.L. Jones, Histology-driven therapy: the importance of diagnostic accuracy in guiding systemic therapy of soft tissue tumors, Int. J. Surg. Pathol. 24 (2016) 5–15.
[71] O.P. Blizniukov, A. Zamogil'naia Ia, [Pleomorphic fibrosarcoma], Vopr. Onkol. 58 (2012) 54–60.
[72] F.X. Dieudonne, A. Marion, E. Hay, P.J. Marie, D. Modrowski, High Wnt signaling represses the proapoptotic proteoglycan syndecan-2 in osteosarcoma cells, Cancer Res. 70 (2010) 5399–5408.
[73] H.R. Contreras, M. Fabre, F. Granes, R. Casaroli-Marano, N. Rocamora, A.G. Herreros, M. Reina, S. Vilaro, Syndecan-2 expression in colorectal cancer-derived HT-29 M6 epithelial cells induces a migratory phenotype, Biochem. Biophys. Res. Commun. 286 (2001) 742–751.
[74] C.M. Vicente, R. Ricci, H.B. Nader, L. Toma, Syndecan-2 is upregulated in colorectal cancer cells through interactions with extracellular matrix produced by stromal fibroblasts, BMC Cell Biol. 14 (2013) 25.
[75] J.J. Essner, E. Chen, S.C. Ekker, Syndecan-2, Int. J. Biochem. Cell Biol. 38 (2006) 152–156.
[76] A. Bretscher, D. Reczek, M. Berryman, Ezrin: a protein requiring conformational activation to link microfilaments to the plasma membrane in the assembly of cell surface structures, J. Cell Sci. 110 (Pt 24) (1997) 3011–3018.
[77] R. Gary, A. Bretscher, Ezrin self-association involves binding of an N-terminal domain to a normally masked C-terminal domain that includes the F-actin binding site, Mol. Biol. Cell 6 (1995) 1061–1075.
[78] R. Zhou, L. Zhu, A. Kodani, P. Hauser, X. Yao, J.G. Forte, Phosphorylation of ezrin on threonine 567 produces a change in secretory phenotype and repolarizes the gastric parietal cell, J. Cell Sci. 118 (2005) 4381–4391.
[79] Y.F. Chen, C.Y. Chou, R.J. Wilkins, J.C. Ellory, D.B. Mount, M.R. Shen, Motor protein-dependent membrane trafficking of KCl cotransporter-4 is important for cancer cell invasion, Cancer Res. 69 (2009) 8585–8593.
[80] F. Naftolin, L.M. Garcia-Segura, T.L. Horvath, A. Zsarnovszky, N. Demir, A. Fadiel, C. Leranth, S. Vondracek-Klepper, C. Lewis, A. Chang, A. Parducz, Estrogen-induced hypothalamic synaptic plasticity and pituitary sensitization in the control of the estrogen-induced gonadotrophin surge, Reprod. Sci. 14 (2007) 101–116.
[81] Y. Saygideger-Kont, T.Z. Minas, H. Jones, S. Hour, H. Celik, I. Temel, J. Han, N. Atabey, H.V. Erkizan, J.A. Toretsky, A. Uren, Ezrin enhances EGFR signaling and modulates erlotinib sensitivity in non-small cell lung cancer cells, Neoplasia 18 (2016) 111–120.
[82] S. Shannon, D. Jia, I. Entersz, P. Beelen, M. Yu, C. Carcione, J. Carcione, A. Mahtabfar, C. Vaca, M. Weaver, D. Shreiber, J.D. Zahn, L. Liu, H. Lin, R.A. Foty, Inhibition of glioblastoma dispersal by the MEK inhibitor PD0325901, BMC Cancer 17 (2017) 121.